

See discussions, stats, and author profiles for this publication at: <https://www.researchgate.net/publication/42637855>

# Surface Energy and Wettability of Spin-Coated Thin Films of Lignin Isolated from Wood

ARTICLE *in* LANGMUIR · MARCH 2010

Impact Factor: 4.46 · DOI: 10.1021/la1003337 · Source: PubMed

---

CITATIONS

38

---

READS

44

## 2 AUTHORS:



[Shannon M Notley](#)

Australian National University

48 PUBLICATIONS 1,010 CITATIONS

[SEE PROFILE](#)



[Magnus Norgren](#)

Mid Sweden University

62 PUBLICATIONS 885 CITATIONS

[SEE PROFILE](#)

## Surface Energy and Wettability of Spin-Coated Thin Films of Lignin Isolated from Wood

Shannon M. Notley<sup>\*,†</sup> and Magnus Norgren<sup>‡</sup>

<sup>†</sup>*Department of Applied Mathematics, Research School of Physics and Engineering, Australian National University, Canberra 0200 ACT, Australia, and* <sup>‡</sup>*Department of Natural Sciences, Engineering and Mathematics, Fibre Science and Communication Network, Mid Sweden University, SE-851 70 Sundsvall, Sweden*

Received July 24, 2009

The surface energy of lignin films spin-coated onto oxidized silicon wafer has been determined from contact angle measurements of different test liquids with varying polar and dispersive components. Three different lignin raw materials were used, a kraft lignin from softwood, along with milled wood lignin from softwood and hardwood. Infrared and <sup>31</sup>P NMR spectroscopy was used to identify any major functional group differences between the lignin samples. No significant difference in the total solid–vapor surface energy for the different lignin films was observed; however, the polar component for the kraft lignin was much greater than for either of the milled wood lignin samples consistent with the presence of carboxyl groups and higher proportion of phenolic hydroxyl groups as shown by quantitative <sup>31</sup>P NMR on the phosphorylated samples. Furthermore, the total surface energy of lignin of 53–56 mJ m<sup>−2</sup> is of a similar magnitude to cellulose, also found in the wood cell wall; however, cellulose has a higher polar component leading to a lower contact angle with water and greater wettability than the milled wood lignin. Although lignin is not hydrophobic according to the strictest definition of a water contact angle greater than 90°, water may only be considered a partially wetting liquid on a lignin surface. This supports the long-held belief that one of the functions of lignin in the wood cell wall is to provide water-proofing to aid in water transport. Furthermore, these results on the solid–vapor surface energy of lignin will provide invaluable insight for many natural and industrial applications including in the design and manufacture of many sustainable products such as paper, fiberboard, and polymer composite blends.

### Introduction

Lignin is one of the most abundant naturally occurring polymeric materials chiefly found in the cell wall of woody tree species.<sup>1,2</sup> The chemical structure of lignin is difficult to define, not in the least due to the significant differences in structure when comparing sources, particularly between softwoods and hardwoods. However, in general terms, it is based upon the phenylpropane subunit with some substituent groups linked together through the dehydrogenation polymerization of these monolignols giving rise to a branched amorphous structure.<sup>3–5</sup> The difficulty in determining the lignin macromolecular architecture arises due to the procedures that are undertaken in order to isolate it from the wood fiber wall, which almost inevitably causes some structural changes, depolymerization or introduction of non-native chemical species upon cleavage of bonds.<sup>6,7</sup> While the analysis of these isolated samples has led to a greater understanding of lignin, it is still not possible to directly study naturally occurring lignin in its unaltered form, although some extraction procedures are more benign than others. Milled wood lignin, isolated through the ball milling of wood followed by solvent extraction, is considered to be

the closest to lignin in its natural state. There are a few non-native chemical species introduced during this process; some depolymerization may be expected. Lignin isolated from spent pulping liquors can be significantly degraded and have a large amount of introduced chemical groups such as carboxyl groups (kraft lignin isolated from black liquor during the kraft pulping process) or sulfonate groups (lignosulfonates isolated from liquor during the sulfite pulping process).<sup>2</sup> With such chemical moieties, it may reasonably be expected that the interfacial properties of lignin will be drastically altered, not in the least due to their increased solubility under various aqueous solution conditions.

There is a growing body of literature on the use of model lignin surfaces for the study of many physicochemical phenomena relevant to both the natural and industrial world.<sup>8–20</sup> Such lignin films have been prepared in many different ways including

\*Corresponding author. E-mail: shannon.notley@anu.edu.au. Tel: +61 261257583. Fax: +61 261250732.

(1) Freudenberg, K.; Neish, A. C. *Constitution and biosynthesis of lignin*; Springer-Verlag: New York, 1968.

(2) Sjöström, E. *Wood Chemistry: Fundamental and Applications*; Academic Press: London, 1993; Chapter 4.

(3) Sarkanen, K. V.; Ludwig, C. H. *Lignin, Occurrence, Formation, Structure and Reactions*; Wiley-Interscience: New York, 1971.

(4) Boerjan, W.; Ralph, J.; Baucher, M. *Annu. Rev. Plant Biol.* **2003**, *54*, 519–546.

(5) Vanholme, R.; Morreel, K.; Ralph, J.; Boerjan, W. *Curr. Opin. Plant Biol.* **2008**, *11*(3), 278–285.

(6) Gellerstedt, G.; Lindfors, E. *Holzforchung* **1984**, *38*, 151–158.

(7) Chakar, F. S.; Ragauskas, A. J. *Ind. Crops Prod.* **2004**, *20*(2), 131–141.

(8) Lee, S. B.; Luner, P. *Tappi J.* **1972**, *55*, 116.

(9) Constantino, C. J. L.; Juliani, L. P.; Botaro, V. R.; Balogh, D. T.; Pereira, M. R.; Ticianelli, E. A.; Curvelo, A. A. S.; Oliveira, O. N. J. *Thin Solid Films* **1996**, *284–285*, 191–194.

(10) Constantino, C.; Dhanabalan, A.; Cotta, M.; Pereira-da-Silva, M. R.; Curvelo, A.; Oliveira, O. N. J. *Holzforchung* **2000**, *54*(1), 55–60.

(11) Micic, M.; Jeremic, M.; Radotic, K.; Mavers, M.; Leblanc, R. M. *Scanning* **2000**, *22*(5), 288–294.

(12) Micic, M.; Benitez, I.; Ruano, M.; Mavers, M.; Jeremic, M.; Radotic, K.; Moy, V.; Leblanc, R. M. *Chem. Phys. Lett.* **2001**, *347*(1–3), 41–45.

(13) Pasquini, D.; Balogh, D. T.; Antunes, P. A.; Constantino, C. J. L.; Curvelo, A. A. S.; Aroca, R. F.; Oliveira, O. N. J. *Langmuir* **2002**, *18*(17), 6593–6596.

(14) Pasquini, D.; Balogh, D. T.; Oliveira, O. N. J.; Curvelo, A. A. S. *Colloids Surf., A* **2005**, *252*(2–3), 193–200.

(15) Norgren, M.; Notley, S. M.; Majtnerova, A.; Gellerstedt, G. *Langmuir* **2006**, *22*(3), 1209–1214.

(16) Notley, S. M.; Norgren, M. *Langmuir* **2006**, *22*(26), 11199–11204.

(17) Tammelin, T.; Osterberg, M.; Johansson, L. S.; Laine, J. *Nordic Pulp Paper Res. J.* **2006**, *21*, 444–450.

(18) Norgren, M.; Gardlund, L.; Notley, S. M.; Htun, M.; Wagberg, L. *Langmuir* **2007**, *23*, 3737–3743.

evaporation of solution,<sup>8,12</sup> the Langmuir–Blodgett technique,<sup>9,10</sup> as well as spin-coating of a lignin solution onto a solid supporting substrate.<sup>15–20</sup> Furthermore, many different sources or isolation techniques of lignin have been investigated from the relatively unaltered milled wood lignin to lignin isolated from black liquor during the kraft pulping process. For a summary, the interested reader is referred elsewhere.<sup>15</sup> These variously prepared films have also been used to study the interaction of lignin with different species including cellulose<sup>16</sup> and other wood extractive materials<sup>17,19</sup> and soft matter such as polymers and polyelectrolytes.<sup>18,20</sup> A key factor for success has been the ability to control the thickness and roughness of the lignin films. Such smooth films are ideal for use in measuring the interaction with liquids, particularly in determining contact angles, which may then be used to calculate the surface energy.

Understanding the surface energy and wettability of lignin is important in a number of natural and industrial applications. For example, the implications for the transport of water through the wood fiber is demonstrated by a recent study by Kohonen.<sup>21</sup> In that study, it was demonstrated that structuring of lignin on the fiber lumen wall, of species that are considered drought tolerant, enhanced the flow of water through the tracheid, a condition only possible if the wall is hydrophilic. Furthermore, it has often been suggested that one of the major roles of lignin in the plant cell wall is to impart hydrophobicity and hence provide water-proofing and aid in water transport through the fiber wall.<sup>2,3,22</sup> Another area where knowledge of the surface energy may prove useful is in soil chemistry. Lignin fragments remain in the soil long after the polysaccharides decay at the end of the lifecycle of trees. Thus, lignin contributes significantly to the humus and hence the penetration of water into the subsoil regions will be directly influenced by the wettability of lignin.

In terms of industrial applications, lignin is becoming an increasingly important sustainable material.<sup>23</sup> For many years, wood fibers containing lignin at the interface have been used in products such as paper, cardboard, and engineered wood products. The surface energy of fibers with lignin-rich surface chemistry has a direct influence on the development of capillary forces during the drying and consolidation phases. This will impact the strength of the formed paper sheet. Furthermore, the use of these fibers in products such as medium-density fiberboard requires careful consideration of the interfacial energies in order to develop strong adhesion between the fiber and resin. Recent efforts have sought to expand the use of lignin into other product areas. Lignin and its derivatives are typically used as dispersants for ceramics and as such are localized at the interfacial region. Furthermore, it has been incorporated into other materials applications such as in carbon fiber and polymer blends.<sup>24,25</sup> Hence, it is clear that a full understanding of the interfacial properties of lignin is required.

Lee and Luner conducted a pioneering study on the wettability of molded lignin surfaces<sup>8</sup> showing that the sessile contact angle water made with lignin was about 60°. However, Laschimke concluded that milled wood lignin as well as lignin from the organocell process was “unwettable” even though the contact angle in these measurements was initially around 80°, dropping to

**Table 1. Surface Tension Data for the Test Liquids Used to Determine the Surface Energy of the Lignin Thin Films**

$\gamma$ (mN/m)	water	diiodomethane	formamide
total (measured)	72.8	50.0	57.9
total (literature)	72.8	50.8	58
dispersive	21.8	50.8	39
polar	51	0	19
plus (acid)	25.5	0	2.28
minus (base)	25.5	0	39.6

63° as a function of time.<sup>26</sup> This is significantly less than the minimum of 90° required in the standard definition of hydrophobic material.<sup>27</sup> In this study, the surface energy of model lignin films prepared from raw materials isolated through different means will be investigated. Furthermore, the polar and dispersive components will be determined. From the data presented here, it will be shown that lignin isolated through different means is indeed not hydrophobic according to a standard definition of the surface having a contact angle with water of greater than 90°; rather, water only partially wets the lignin surface.

## Experimental Section

**Materials.** All chemicals used in this study, apart from the lignin samples, were of analytical grade and were supplied by Sigma-Aldrich and used without further purification. Milli-Q water was used in the preparation of the aqueous solution of ammonium hydroxide. The acetone used for the dissolution of some of the lignin samples was analytical-grade. Dried pyridine, cyclohexanol, chromium(III)acetylacetonate, and 2-chloro-4,4,5,5-tetramethyl-1,3,2-dioxaphospholane were supplied by Sigma Aldrich (Sweden), and deuterated chloroform was bought from Larodan (Sweden). For the contact angle measurements, Milli-Q water was used, as well as formamide and diiodomethane, both of which were of analytical grade. The surface tension of the test liquids was determined using the pendant drop method (KSV CAM200, KSV Instruments, Finland) prior to use to ensure purity. The measured surface tension as well as the literature values for the different test liquids is shown in Table 1. All measurements were performed at 20 °C.

**Lignin Samples.** The softwood kraft lignin was isolated from black liquor of wood pulp from *Picea abies*. This is the same material that has been used in previous studies on the surface and physical properties of softwood kraft lignin films.<sup>15,16,18,20</sup> The milled wood samples were provided by Warwick Raverty, CSIRO Australia. The softwood sample was prepared from Radiata Pine and the hardwood from Eucalyptus Regnans according to a previously described method.<sup>28</sup>

**Lignin Phosphitylation Procedure.** The lignin phosphitylation procedure to mark specifically different hydroxyl groups present in the lignin samples for subsequent quantitative <sup>31</sup>P NMR analysis was based on a method thoroughly developed and verified by Argyropoulos and co-workers.<sup>29–33</sup> A solvent mixture (solution A) of dried pyridine and deuterated chloroform mixed in a 1.6/1 v/v ratio was prepared, and molecular sieves (3 Å) were added to minimize the moisture. In a 10 mL flask, 110 mg cyclohexanol and 55 mg chromium(III)acetylacetonate, serving as an internal

(26) Laschimke, R. *Thermochim. Acta* **1989**, *151*, 33–56.

(27) Hunter, R. J. *Introduction to modern colloid science*; Oxford University Press: Oxford, 1993; Chapter 5.

(28) Lindstrom, T.; Wallis, A.; Tulonen, J.; Kolseth, P. *Holzforschung* **1988**, *42*, 225–228.

(29) Argyropoulos, D. S.; Henry, I.; Bolker, H. I.; Heitner, C.; Archipov, Y. *J. Wood Chem. Technol.* **1993**, *13*, 187–212.

(30) Argyropoulos, D. S. *J. Wood Chem. Technol.* **1994**, *14*, 65–82.

(31) Sun, Y.; Argyropoulos, D. S. *J. Pulp and Paper Sci.* **1995**, *21*, J185–J190.

(32) Granata, A.; Argyropoulos, D. S. *J. Agric. Food Chem.* **1995**, *43*, 1538–1544.

(33) Guerra, A.; Filpponen, I.; Lucia, L. A.; Saquing, C.; Baumberger, S.; Argyropoulos, D. S. *J. Agric. Food Chem.* **2006**, *54*, 5939–5947.

(19) Tammelin, T.; Jonhsen, I. A.; Osterberg, M.; Stenius, P.; Laine, J. *Nordic Pulp Paper Res. J.* **2007**, *22*, 93–101.

(20) Notley, S. M.; Norgren, M. *Biomacromolecules* **2008**, *9*, 2081–2086.

(21) Kohonen, M. M. *Langmuir* **2006**, *22*, 3148–3153.

(22) Hon, D. N.; Shiraishi, N. *Wood and Cellulosic Chemistry*; Marcel Dekker: New York, 1991; Chapter 4.

(23) Gandini, A. *Macromolecules* **2008**, *41*, 9491–9504.

(24) Kadla, J. F.; Kubo, S.; Venditti, R. A.; Gilbert, R. D.; Compere, A. L.; Griffith, W. *Carbon* **2002**, *40*(15), 2913–2920.

(25) Kubo, S.; Kadla, J. F. *J. Polym. Environ.* **2005**, *13*(2), 97–105.



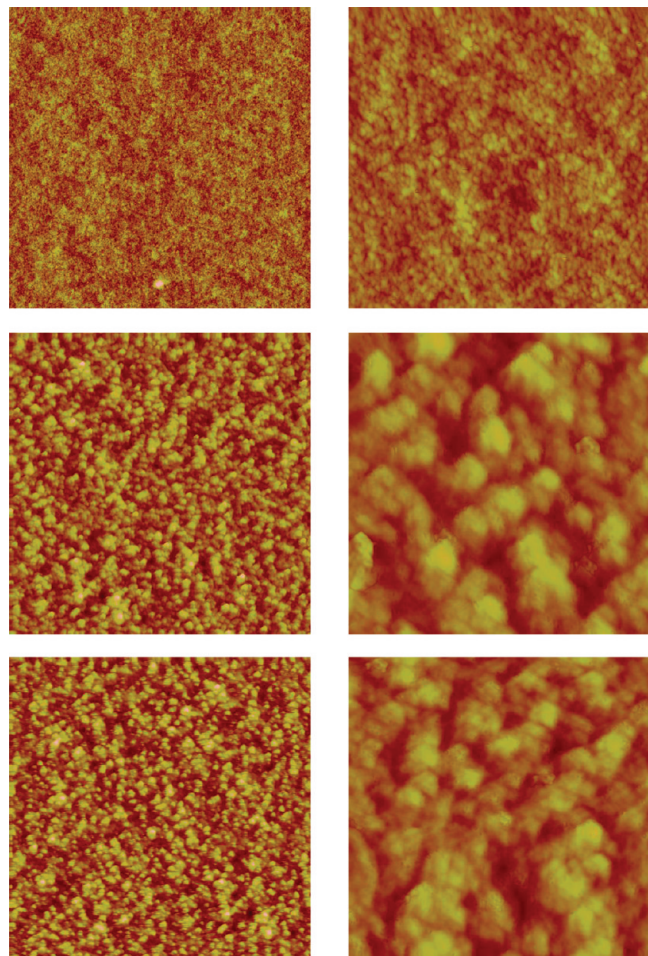


**Figure 1.** AFM noncontact mode height images of lignin thin films prepared by spin-coating. The data scale is  $5\ \mu\text{m} \times 5\ \mu\text{m}$  for the left images and  $1\ \mu\text{m} \times 1\ \mu\text{m}$  for the images on the right. Top images: kraft lignin film, rms roughness of 0.93 nm. Middle images: hardwood milled wood lignin film, rms roughness of 1.38 nm. Bottom images: softwood milled wood lignin film, rms roughness of 1.31 nm.  $z$  scale for all images is 15 nm.

standard and used as a relaxation reagent, respectively, were accurately weighed and diluted to the mark with solution A to create solution B. The lignin samples (40 mg) were accurately weighed into 2 mL volumetric flasks, and 820  $\mu\text{L}$  of solution A was added to each sample. The flasks were sealed with Teflon-lined screw caps and dissolved by thorough mixing during 72 h. Thereafter, the lignin samples were phosphitylated by an addition of 80  $\mu\text{L}$  2-chloro-4,4,5,5-tetramethyl-1,3,2-dioxaphospholane, and the flasks were sealed and shaken to ensure good mixing. In a final step, 100  $\mu\text{L}$  of solution B was added and the flasks were sealed and shaken once again.

**Lignin Film Preparation.** Kraft lignin films were prepared according to the method previously described by Norgren et al.<sup>15</sup> A 1.5% w/w solution of softwood kraft lignin in 1 M  $\text{NH}_4\text{OH}$  was prepared. The lignin was allowed to dissolve in the ammonium hydroxide for 24 h prior to use. This solution was then used in the spin-coating of smooth, thin lignin films onto oxidized silicon wafer (Peregrine Semiconductors Pty Ltd. Sydney, Australia) which were cleaned thoroughly by exposing the surfaces to a 10% w/w solution of NaOH, rinsing with Milli-Q water, and finally subjecting them to a mild water plasma treatment to ensure that the surfaces were fully wetting. The solution was spin-coated onto the silica surfaces for 60 s at 1500 rpm to produce kraft lignin films with a thickness of 50–60 nm as measured using ellipsometry with a refractive index of 1.60.<sup>15</sup> The kraft lignin films were placed

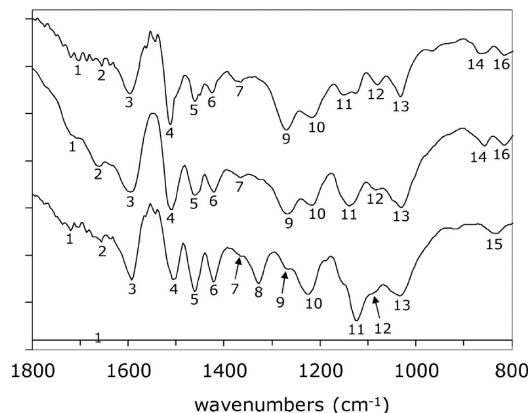


**Figure 2.** FTIR spectra for the softwood kraft lignin sample (top), softwood MWL (middle), and hardwood MWL (bottom). Numbers refer to the peak assignments listed in Table 2.

in Milli-Q water for 2 h. Finally, the lignin surfaces were dried under nitrogen. The contact angle measurements were undertaken within 24 h of the film preparation.

The other samples of lignin were similarly used in the preparation of thin films. However, instead of being dissolved in 1 M  $\text{NH}_4\text{OH}$ , a 9:1 mixture of acetone and water was used. Typically, a 1% w/w solution of the lignin sample was dissolved in the acetone/water mixture before spin-coating onto the oxidized silicon wafers with the same spinning parameters. The thin lignin films were in the thickness range 30–60 nm, depending on the chemistry of the lignin sample. Atomic force microscopy imaging of the films (MFP-3D, Asylum Research, USA), as shown in Figure 1, showed that they were continuous and smooth over a large area (greater than  $25\ \mu\text{m}^2$ ).

**Fourier Transform Infrared (FTIR) Spectroscopy.** FTIR spectra of the lignin samples were measured with a Shimadzu FTIR-8400 in the solid state. KBr pellets with a lignin concentration of about 1% were prepared. Sixteen scans were acquired with a spectral resolution of  $4.0\ \text{cm}^{-1}$ . Shimadzu *IR Solution* software was used to determine the peak position.

**$^{31}\text{P}$  NMR Analysis.** The  $^{31}\text{P}$  NMR analyses were performed in 5 mm NMR precision tubes (Glasser AB, Sweden) on a Bruker Avance 500 MHz NMR spectrometer (Bruker BioSpin, Germany) according to a well-documented procedure.<sup>31–33</sup> The spectrometer settings were as follows: sweep width 6.6 kHz, pulse angle  $45^\circ$ , inverse gated decoupling. The spectra were accumulated with a relaxation delay time of 25 s between successive pulses. All chemical shifts reported are relative to the reaction product of water with the phosphitylation reagents at 132.2 ppm. In the processing of the spectra for the quantitative determinations, an exponential window function with a line broadening of 3 Hz was used.

**Contact Angle Measurements.** Contact angle measurements were undertaken using a KSV CAM200 contact angle goniometer (KSV Instruments, Finland). The contact angle for a minimum of three drops on three different substrates for each type of lignin film was measured. The drop profile was fit by equating the hydrostatic pressure of the drop of a known volume to the Laplace pressure at every point on the drop's curved interface. The advancing contact angle was typically used rather than the sessile drop contact angle method. However, for some cases the sessile drop contact angle was measured as a function of time in order to probe whether the lignin surfaces were taking up the test liquid.

According to the methods outlined below for the determination of surface energy, at least three test liquids with varying polar and dispersive components were used for each surface. Importantly, liquids were chosen that would have no interaction with lignin by careful consideration of the Hansen solubility parameters.<sup>34</sup> If the

(34) Hansen, C. M. *Hansen Solubility Parameters: a user's handbook*, 2nd ed.; CRC Press: Boca Raton, 2007; Chapter 15.

**Table 2. Peaks Observed in the Infrared Spectra and Their Assignments for Softwood Kraft Lignin (SKL), Softwood Milled Wood Lignin (SMWL), and Hardwood Milled Wood Lignin (HMWL)**

peak	SKL peak position (cm <sup>-1</sup> )	SMWL peak position (cm <sup>-1</sup> )	HMWL peak position (cm <sup>-1</sup> )	peak assignment
1	1705	1705	1705	C=O stretching in carbonyl groups
2	1655	1662	1655	C=O stretching in carbonyl groups
3	1597	1593	1593	aromatic ring vibration
4	1512	1508	1504	aromatic ring vibration
5	1462	1462	1462	C–H deformation
6	1427	1423	1423	C–H in plane deformation with aromatic ring stretching
7	1366	1366	1366	phenolic OH and aliphatic C–H in methyl groups
8	-	-	1327	C–O stretching on the syringyl aromatic ring
9	1269	1269	1270	C–O stretching on the guaiacyl aromatic ring
10	1219	1219	1222	C–C and C–O stretching
11	1149	1138	1140	aromatic C–H stretching of the guaiacyl ring
12	1080	1084	1084	C–O deformation of secondary alcohols
13	1034	1030	1034	aromatic C–H in plane deformation
14	860	860	-	aromatic C–H in plane deformation
15	-	-	829	aromatic C–H in plane deformation
16	818	818	-	aromatic C–H in plane deformation

liquid interacts substantially with the lignin polymer substrate, solvent penetration into the surface effectively reduces the contact angle as the drop spreads on a mixed chemistry interface according to equation given by Cassie and Baxter.<sup>35</sup> Literature values for the total Hansen solubility parameter,  $\delta_T$ , of lignin<sup>36–39</sup> are on the order of 22–31 MPa<sup>1/2</sup> depending on the source of the material, which is substantially different from the test liquids which are 19.0, 36.6, and 47.8 MPa<sup>1/2</sup> for diiodomethane, formamide, and water, respectively.<sup>34</sup> For the polymer to be soluble in the solvent, the magnitudes of the  $\delta_T$  for each component need to be well-matched and, furthermore, be of similar strength in terms of hydrogen bonding ability. In this case, lignin can be classed as a weak to moderate hydrogen bonding material, and for three test liquids, formamide is the only solvent of similar strength; however, the  $\delta_T$  is much larger, suggesting very limited interaction with lignin at best. Furthermore, calculation of the Flory–Huggins interaction parameter,  $\chi_{12}$ , based on the Hildebrand solubility,<sup>40</sup> indicate values of greater than 0.5 for all solvents demonstrating nonsolvency of lignin in diiodomethane, formamide, and water.

**Surface Energy Calculations.** The surface energy of the different lignin films was determined following two different methods, that of Fowkes,<sup>41</sup> which considers the polar and dispersive components, and that of van Oss,<sup>42</sup> which subsequently breaks down the polar component into acid and base contributions. These two methods will be detailed below.

The Fowkes method<sup>41</sup> for determining the polar and nonpolar components of the surface energy of the lignin films uses a geometric mean of the polar and dispersive to combine their contributions, which when combined with the Young equation gives eq 1.

$$\gamma_l(1 + \cos \theta) = 2(\sqrt{\gamma_l^p \gamma_s^p} + \sqrt{\gamma_l^d \gamma_s^d}) \quad (1)$$

Equation 1 can be rearranged, as done by Owens and Wendt,<sup>43</sup> to give the form as shown in eq 2 where the components of the solid surface energy are easily determined from measurement of

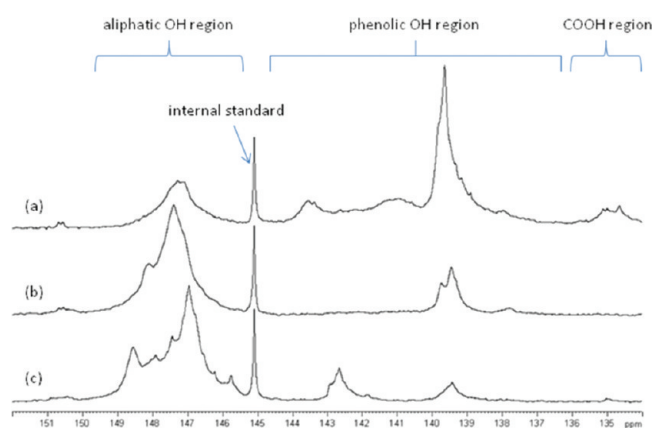


**Figure 3.** Quantitative <sup>31</sup>P NMR spectra of softwood kraft lignin (a), softwood MWL (*Pinus radiata*) (b), hardwood MWL (*Eucalyptus Regnans*) (c). The lignin samples were phosphitylated with 2-chloro-4,4,5,5-tetramethyl-1,3,2-dioxaphospholane and the internal standard used was cyclohexanol.

the contact angle for liquids with accurately known polar and dispersive components of their surface tension.

$$\frac{\gamma_l(1 + \cos \theta)}{2\sqrt{\gamma_l^d}} = \sqrt{\gamma_s^p \left( \frac{\gamma_l^p}{\gamma_l^d} \right)} + \sqrt{\gamma_s^d} \quad (2)$$

The method of van Oss<sup>42</sup> was also used to determine the solid surface energy components; however, the dispersive contribution was further broken down into acid and base components as shown in eq 3 below where the superscripts + and – refer to the dispersive acid and base components, respectively. There is, however, some conjecture as to the validity of this approach as there are significant differences in the literature values for the acid and base components. Contact angle measurements for a minimum of three test liquids is required when using this method as there are three unknown variables.

$$\frac{(1 + \cos \theta)\gamma_l}{2} = \sqrt{\gamma_s^d \gamma_l^d} + \sqrt{\gamma_s^+ \gamma_l^+} + \sqrt{\gamma_s^- \gamma_l^-} \quad (3)$$

## Results and Discussion

The spin-coated lignin surfaces were first imaged to ensure that the preparation procedure resulted in smooth and continuous films. Figure 1 shows AFM images over 1 μm<sup>2</sup> and 25 μm<sup>2</sup> for the

(35) De Gennes, P. G.; Brochard-Wyart, F.; Quere, D. *Capillarity and Wetting Phenomena: Drops, Bubbles, Pearls, Waves*; Springer: Berlin, 2003; Chapter 9.

(36) Schuerch, C. *J. Am. Chem. Soc.* **1952**, *74*, 5061–5067.

(37) Brown, W. J. *Appl. Polym. Sci.* **1967**, *11*, 2381–2396.

(38) Kelley, S. S.; Rials, T. G.; Glasser, W. G. *J. Mater. Sci.* **1987**, *22*, 617–624.

(39) Hansen, C. M.; Bjorkman, A. *Holzforschung* **1998**, *52*, 335–344.

(40) Rubinstein, M.; Colby, R. H. *Polymer Physics*; Oxford University Press: New York, 2003; Chapter 4.

(41) Fowkes, F. M. *Ind. Eng. Chem.* **1964**, *56*, 40.

(42) van Oss, C. J. *Interfacial Forces in Aqueous Media*; Marcel Dekker: New York, 1994.

(43) Owens, D. K.; Wendt, R. C. *J. Appl. Polym. Sci.* **1969**, *13*, 1741.

**Table 3. Hydroxyl Content (mmol/g) in Lignin Samples Determined by Quantitative  $^{31}\text{P}$  NMR Analysis**

sample	guaiacyl and demethylated phenolic	syringyl phenolic	condensed phenolic	tot. phenolic hydroxyls	tot. aliphatic hydroxyls	carboxyl groups
Kraft lignin	2.7	NA <sup>a</sup>	1.0	3.7	1.9	0.48
softwood MWL <sup>b</sup>	0.93	NA	0.02	0.95	4.0	NA
hardwood MWL <sup>c</sup>	0.35	0.60	NA	0.95	5.0	0.03

<sup>a</sup> NA, not applicable. <sup>b</sup> *Pinus radiata*. <sup>c</sup> *Eucalyptus Regnans*.

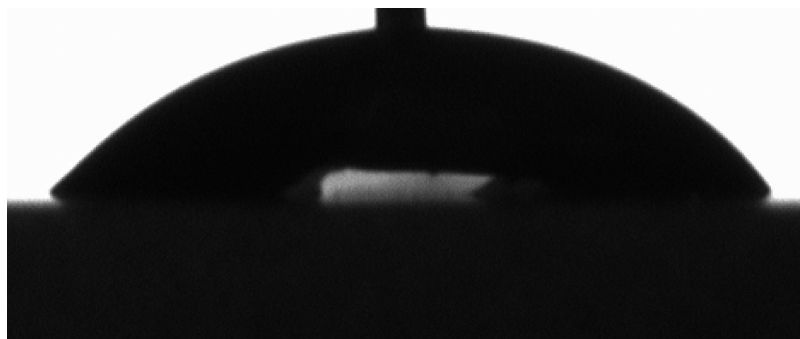


**Figure 4.** Typical example of a sessile drop of water on a softwood milled wood lignin film. Contact angles used in this study were determined from the advancing angle as the drop size increased.

three different lignin films used in this study. All samples have low roughness and are free from any cracks or large holes which may significantly influence the contact angle measurements. The root-mean-square roughness of the films is on a nanometer scale, and as such, this structural heterogeneity is not expected to affect the advancing contact angle of the test liquids. Furthermore, there are no significant differences between the morphology of the milled wood lignin films as shown in Figure 1. However, the kraft lignin films show much smaller aggregates on the surface and hence are much smoother. This is most likely due to the difference in solubility of the kraft lignin in ammonium hydroxide to the milled wood lignin in the acetone–water mixture. The ratio of real surface area to projected surface area is less than 1.01, indicating that the surface roughness should not have a significant impact on the observed contact angle.<sup>35</sup>

FTIR spectra for each of the lignin samples were measured and the fingerprint spectral regions are shown in Figure 2. The major peak assignments for the functional groups are listed in Table 2. The position of the peaks of the major functional groups as well as their intensity is in agreement with previously published results on lignin.<sup>22,44,45</sup>

As can be found in Figure 2 and Table 2, evidence of carbonyl stretching is observed for all the samples at  $1720\text{--}1650\text{ cm}^{-1}$ . It has been well established that carboxylic acid groups are introduced to kraft lignin during the pulping process. However, since the FTIR analysis provides only qualitative information about the chemical functionalities of the lignin samples, further structural elucidation of the presence of major chemical functionalities important for the physical features of the samples, such as the surface energy, was also performed. The lignin samples were phosphitylated and analyzed by quantitative  $^{31}\text{P}$  NMR to determine the amounts of different hydroxyl groups.<sup>29–33</sup> Figure 3 shows the NMR spectra for each of the lignin samples under investigation, while Table 3 provides the quantitative analysis of hydroxyl group content.

As can be seen from the data in Table 3, the number of phenolic groups is much higher in the kraft lignin than in the MWLs. The

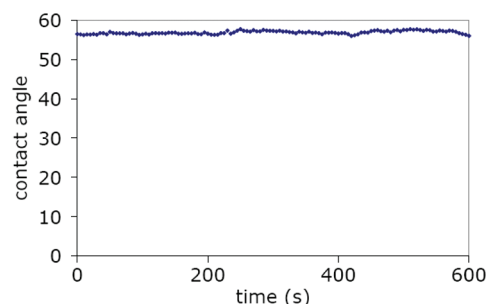


**Figure 5.** Sessile drop contact angle of water on a hardwood milled wood lignin film as a function of time.

MWLs have the same total amount of phenolic groups, but the origin is different; syringyl phenolic as well as guaiacyl phenolic moieties are present in the hardwood lignin, but only guaiacyl phenolic units can be seen in the softwood lignin. Moreover, compared with the softwood MWL, the hardwood MWL sample has some higher amounts of aliphatic hydroxyls, and trace amounts of carboxylic acid groups can be observed in the spectra of the latter sample. The kraft lignin shows a significant signal confirming the presence of carboxyl groups in this sample, whereas the softwood and hardwood MWLs show no or only traces of carboxyl groups, respectively.

Contact angles for the three different test liquids, water, diiodomethane, and formamide, were measured for each of the lignin films. The measurements were performed in a saturated vapor environment to minimize the loss in volume of the drop as a function of time. The advancing contact angles were typically used in the calculations of the solid lignin film surface energy. Figure 4 shows an example of a water droplet on a softwood MWL film from which the contact angle was determined. The contact angle of a sessile drop was used to investigate if there was any significant time dependence which may be due to liquid uptake in the film due to solubility or film porosity. Such scenarios would result in the liquid effectively spreading on top of itself while the drop is growing in the advancing measurements, which leads to a significantly smaller value of the contact angle. Figure 5 shows the measured contact angle for a sessile drop of

(44) Michell, A. J. *Aust. J. Chem.* **1966**, *19*, 2285–2298.

(45) Kubo, S.; Kadla, J. F. *Biomacromolecules* **2005**, *6*, 2815–2821.



**Table 4. Measured Advancing Contact Angles of the Test Liquids on the Spin-Coated Lignin Thin Films**

surface	water	diiodomethane	formamide
softwood Kraft	46° ± 1.5°	51° ± 0.5°	20° ± 0.5°
softwood MWL	52.5° ± 1°	23° ± 1°	19.5° ± 0.5°
hardwood MWL	55.5° ± 1.5°	27° ± 1°	21.5° ± 0.5°

**Table 5. Surface Energy, Including Polar and Dispersive Components, of Model Lignin Films Calculated Using the Method of Fowkes<sup>41</sup>**

energy (mJ m <sup>-2</sup> )	softwood kraft	softwood MWL	hardwood MWL	REAX 31 <sup>8</sup>
$\gamma_T$	57.1	58.8	57.0	52.5
$\gamma_d$	33.7	44.5	43.9	43.5
$\gamma_p$	23.4	14.3	13.1	9.0

water on a hardwood MWL film as a function of time. As can be seen from these data, only a small reduction in the contact angle is observed over 10 min, most likely due to the slowly decreasing volume of the drop as liquid evaporates, resulting in an effective change in the measurement regime from a sessile measurement to a receding contact angle measurement. After the drop was removed from the surface, there was no evidence to suggest that the lignin film imbibed any of the test liquids.

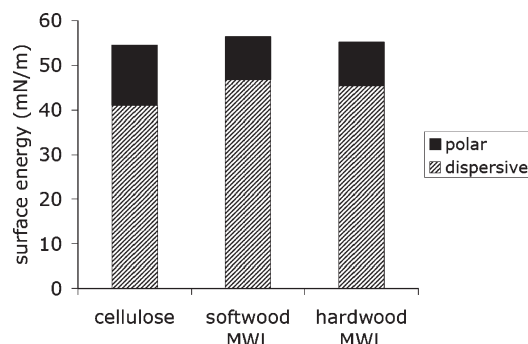
Table 4 summarizes all of the measured advancing contact angles for the different liquids on the spin-coated lignin thin films. Importantly, water partially wet all of the lignin films. The data from the advancing contact angles were used to calculate the surface energies of lignin from the different sources and isolation methods. The polar and dispersive contributions to the surface energy of lignin were determined using the Fowkes method as described by eq 2. The calculated solid surface energy values are shown in Table 5.

Interestingly, the data shown in Table 5 demonstrate that the total surface energy of the solid lignin thin films calculated using this method is relatively insensitive to the origin of the lignin as well as how it was isolated. However, there is a significant difference in the polar and dispersive components between the kraft lignin and the milled wood lignin samples. The softwood kraft lignin thin films showed a much higher polar component of the total surface energy than either of the MWL films whether prepared from softwood or hardwood lignin. This is due to the introduction of many highly polar chemical moieties during the kraft pulping process which have previously been shown to remain in the film after spin-coating.<sup>15</sup> Of particular importance are the charged carboxyl groups as well as the increased number of phenolic groups which give rise to the increased solubility of the lignin at high pH. Furthermore, the data in Table 5 show that the polar and dispersive contributions to the surface energy for both MWL samples are within the experimental error. This suggests that the proportion of the different monomer units which make up the hardwood and softwood lignin polymer do not significantly influence the overall surface energy of lignin.

The data for the surface energy of lignin from the previous study by Lee and Luner<sup>8</sup> is also included in Table 5. The total surface energy is lower for the sample used in that study, REAX 31 lignin, with the major difference being a somewhat lower polar component. However, the differences overall are minimal which suggests that the preparation procedures for the lignin surfaces do not significantly influence the surface energy. It is important to note that stable contact angle measurements were not possible in this earlier study, that is, there was a significant decrease in the contact angle with time most probably due to the porous nature of the molded lignin surfaces.

**Table 6. Surface Energy, with the Dispersive Components Broken Down into Acid and Base Contribution, of Model Lignin Films Calculated Using the Method of van Oss<sup>42</sup>**

energy (mJ m <sup>-2</sup> )	softwood kraft	softwood MWL	hardwood MWL
$\gamma_T$	53.2	56.4	55.2
$\gamma_d$	33.7	46.8	45.4
$\gamma_{p+}$	4.1	1.5	1.7
$\gamma_{p-}$	23.3	15.6	14.1
$\gamma_{p\text{ tot}}$	19.5	9.6	9.8

**Figure 6.** Total surface energy of cellulose and lignin model films divided into their polar and dispersive components. Data for cellulose taken from Eriksson et al.<sup>46</sup>

The acid and base contributions to the polar component of the surface energy were also determined from contact angle measurements on the three lignin films according to the method of van Oss.<sup>42</sup> For all three lignin films, the basic component of the polar surface energy dominates over the acidic component as shown in Table 6. This may be expected as most materials containing significant phenolic and methoxyl chemical groups behave similarly with strong electron donating capacity and hence have the ability to participate in polar interactions with acidic species.

From the data presented in Tables 5 and 6, it is clear that the surface energy of the milled wood lignin samples is not significantly influenced by the source of the material. MWL is considered to be most like the naturally occurring lignin found in wood fiber of all the variously available preparation and isolation methods, as it has been chemically modified the least. It is important to note that the total surface energy for both MWL is not significantly different from the other major component of the wood fiber cell wall cellulose. Literature values for the total surface energy of cellulose are on the order of 54.5 mJ m<sup>-2</sup>; however, the contact of water on cellulose films is typically much lower at around 20°. <sup>42</sup> A similar analysis of contact angle data was recently performed on model cellulose thin films<sup>46</sup> and it was found that, while the surface energy of cellulose was dominated by dispersive interactions, the polar component was higher than the MWL films studied here. The comparison between the surface energy components for these two wood biopolymers is demonstrated in Figure 6.

While the total solid–vapor surface energy of cellulose and lignin is of similar magnitude, the contact angle with water for these materials clearly shows that cellulose has a higher wettability than lignin. However, it is important to note that, for both materials, water will partially wet the surfaces. The data presented here in this study, along with numerous previous studies, could hence cast doubt on one speculated role of

(46) Eriksson, M.; Notley, S. M.; Wagberg, L. *Biomacromolecules* **2007**, *8*, 912–919.

lignin in the wood cell wall. It is often thought that lignin aids in the transport of water through the tracheid by providing effective waterproofing; however, the contact angle data presented here suggest that this cannot be the case, at least not from a strict chemical viewpoint, i.e., without considering the effects of surface roughness/structural distribution on the contact angle. It is possible though that the lignin samples used in this study do have some chemical changes due to the milling and extraction process, which may cause an increase in water wettability. This is obvious for the kraft lignin where it is well-known that many polar groups are introduced by the action of hydroxide and hydrogen sulfide, which is clearly supported by the  $^{31}\text{P}$  NMR data presented in Table 3. However, the isolation and extraction of the MWL samples is usually considered to be benign. It seems as though, by considering Young's equation, that the solid–liquid interfacial energy for cellulose and lignin must hence be significantly different for the interaction of water on these surfaces and is the dominant factor in determining the wettability for this case. Thus, the challenge still remains in studying the wettability of lignin with a range of materials. This paper has only considered very smooth lignin surfaces. The structuring of the lignin within the wood fiber, particularly the lumen, will obviously have a major impact on the wettability.<sup>21</sup> However, a better understanding of the native structure will eventually provide valuable insight.

## Conclusions

The polar and dispersive components of the solid–vapor surface energy for three types of lignin thin films was determined from the measurements of contact angles of various test liquids on the model surfaces. The surface energy was in the range  $53\text{--}56\text{ mJ m}^{-2}$  for the milled wood lignin films and the kraft lignin film. The polar component of the surface energy of the kraft lignin films was significantly higher than that of the milled wood lignin samples due to the introduction of charged chemical groups in the isolation process. Interestingly, the surface energy of all samples determined here was remarkably similar to that of cellulose, the other major component in the wood cell wall. However, the contact angle of water on cellulose is much lower in comparison. This suggests that the difference in the solid–liquid interfacial energy dominates the wettability of water on cellulose and lignin. This has important implications for the understanding of water transport in trees as well as the development of capillary forces during the production of paper, and is also a piece of a puzzle for future utilization of lignin as component in the development of new sustainable materials.

**Acknowledgment.** Göran Gellerstedt and Andrea Majtnerova, KTH, are thanked for providing the softwood kraft lignin sample. Warwick Raverty, CSIRO (ENSIS) is thanked for providing the milled wood lignin samples. Vance Lawrence, Research School of Chemistry, ANU, is thanked for assistance with the FTIR measurements.